



## A modular display system for insect behavioral neuroscience

Michael B. Reiser<sup>a,\*</sup>, Michael H. Dickinson<sup>b</sup>

<sup>a</sup> Department of Computation and Neural Systems, Caltech, MC 138-78, Pasadena, CA 91125, USA

<sup>b</sup> Department of Bioengineering, Caltech, MC 138-78, Pasadena, CA 91125, USA

Received 18 September 2006; received in revised form 22 July 2007; accepted 23 July 2007

### Abstract

Flying insects exhibit stunning behavioral repertoires that are largely mediated by the visual control of flight. For this reason, presenting a controlled visual environment to tethered insects has been and continues to be a powerful tool for studying the sensory control of complex behaviors. To create an easily controlled, scalable, and customizable visual stimulus, we have designed a modular system, based on panels composed of an  $8 \times 8$  array of individual LEDs, that may be connected together to 'tile' an experimental environment with controllable displays. The panels have been designed to be extremely bright, with the added flexibility of individual-pixel brightness control, allowing experimentation over a broad range of behaviorally relevant conditions. Patterns to be displayed may be designed using custom software, downloaded to a controller board, and displayed on the individually addressed panels via a rapid communication interface. The panels are controlled by a microprocessor-based display controller which, for most experiments, will not require a computer in the loop, greatly reducing the experimental infrastructure. This technology allows an experimenter to build and program a visual arena with a customized geometry in a matter of hours. To demonstrate the utility of this system, we present results from experiments with tethered *Drosophila melanogaster*: (1) in a cylindrical arena composed of 44 panels, used to test the contrast dependence of object orientation behavior, and (2) above a 30-panel floor display, used to examine the effects of ground motion on orientation during flight. © 2007 Elsevier B.V. All rights reserved.

**Keywords:** Insect vision; *Drosophila*; Flight control; Visually mediated behavior; Optic flow

### 1. Introduction

Conventional display technologies, such as cathode ray tubes and liquid crystal displays, are not well-suited for use as stimuli for insect experiments because their refresh rates are typically much slower than the flicker fusion rates of insect visual systems (Miall, 1978). In this paper we present a display system, based on LEDs, that was designed as a stimulus for the fly visual system. Because LEDs can be rapidly refreshed, the displays can be used to present apparent motion stimuli. The system we have developed reinforces the many advantages of modern electronic technologies in enabling powerful, low-cost laboratory instruments that are a welcomed addition to the neurobiologist's toolkit. This new display technology is described and the usefulness of the tool is demonstrated by presenting results from behavioral experiments with *Drosophila*.

Using visual stimuli in conjunction with behavioral studies of the visuomotor responses of insects is an established laboratory technique with a rich history. Early experiments used patterned cylinders that were mechanically rotated to provide a moving visual stimulus. Behavior observed using these type of experiments led to the development of the principle of reafference (Von Holst and Mittelstaedt, 1950), the formulation of the Hassenstein–Reichardt model for visual motion detection (Reichardt, 1961), and the discovery of the syndirectional optomotor response, measured in flies using a torque compensator (Götz, 1964). This technique continues to find use in the most recent studies of visual learning in flies (Liu et al., 2006). Revolving static patterns are an appropriate stimulus for studying the response of flies to coherent rotatory motion, but even with many creative modifications, large classes of motion stimuli cannot be presented with such a system. To develop a model for the response of *Drosophila* to progressive and regressive motion, Götz (1968) used two independently controlled projectors to present moving stimuli to each eye. Even better spatial control of the motion stimulus was necessary for electrophysiological investigations of motion sensitive neurons in blowflies; Hausen (1982) used pattern projectors mounted on a gimbal and Krapp

\* Corresponding author. Present address: Howard Hughes Medical Institute, Janelia Farm Research Campus, Ashburn, VA 20147, USA.  
Tel.: +1 571 209 4181; fax: +1 571 209 4917.

E-mail address: reisermb@janelia.hhmi.org (M.B. Reiser).

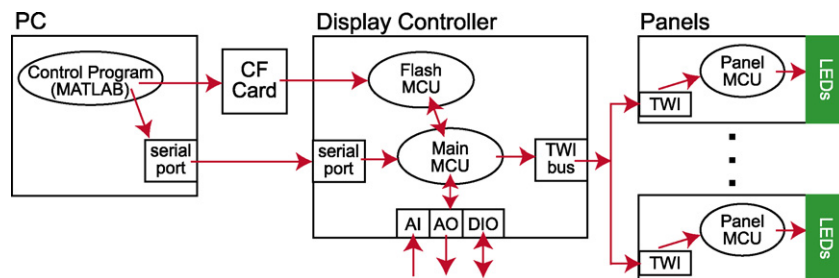


Fig. 1. The panel-based display system has been designed to rapidly transmit pattern data from storage to the panels. Patterns are created using custom-written software, and stored on a CompactFlash (CF) card. The display controller contains two microcontroller units (MCUs). The flash MCU reads pattern data from the CF card and sends it to the main MCU. The main MCU receives directives from the PC control program over the serial port and maintains the timing of display updates. The main MCU communicates with external devices over Analog Input (AI), Analog Output (AO), and Digital Input/Output (DIO) ports. Once fetched from the flash MCU, the updated pattern frames are sent out to the individual panels over the Two Wire Interface (TWI). On each panel, an MCU receives the pattern data and refreshes the display of LEDs.

and Hengstenberg (1997) developed an elaborate system consisting of multiple servomotors each moving a small dot attached to stage that can be positioned at various locations relative to the fly's retina. Continuing the practice of incorporating newer electronic technologies with enhanced performance, LED-based systems have recently come into standard usage (Strauss et al., 1997; Lehmann and Dickinson, 1997; Lindemann et al., 2003). Unlike systems used in the past, LED-based systems are capable of displaying panoramic visual motion with suitable spatial and temporal control. The system we present in this paper is not the result of an effort to design one specific stimulus-generating apparatus for flies. Rather, the system makes it possible to introduce an affordable and programmable visual stimulus into virtually any fly behavior experiment. The system has been designed to address the challenges of conducting experiments on insect vision—it accommodates electrophysiological recordings, can be configured into many geometries, supports high rates of pattern refresh, and can deliver bright visual stimuli over a wide range of contrast levels.

## 2. Methods

### 2.1. System overview

The display system has been designed around programmable modules to allow for the rapid development of behaviorally relevant visual stimuli. The files needed to build, program, and control the system are available from the project web site.<sup>1</sup> The system consists of three major components:

- PC software—set of tools for generating and storing patterns and conducting experiments by communicating with the display controller.
- Panel display controller (PDC)—dual microcontroller circuit that retrieves pattern data from memory, sends the appropriate segment to each panel, and receives commands from the PC control program.

- Panels—individually addressed display modules with an  $8 \times 8$  dot matrix array of LEDs, and supporting electronics to locally refresh the display (photographs in Fig. 2A).

The general flow of information is shown in Fig. 1. A display is constructed using a circuit board as an electrical and architectural substrate to which panels are connected. This circuit board is powered separately from the PDC, and contains a connection from the PDC, through which pattern data pass onto the panels. In the results presented, two types of displays are used: a cylindrical flight arena (Fig. 2B) and a planar 'screen' (Fig. 2C), although many other display geometries are possible.

### 2.2. PC software components

The display system is supported by a set of software tools that run on a Windows-based PC. The software, all developed and run under MATLAB (Mathworks, Inc.), serves two distinct functions: (1) the creation, testing, and storage of patterns, and (2) the coordination of the PDC output while the system is in operation. The overall system has been designed to eliminate the need for low-latency computations to originate on the PC. The essential timing operations for transmitting pattern data to the display are implemented on the PDC, while the less timing-critical functions are implemented on the PC using a comprehensible, high-level language. The complex task of rendering pattern data is not performed while the display is being updated. Rather all patterns are compiled in advance, and stored on an inexpensive CompactFlash (CF) card, which is then transferred to the PDC.

#### 2.2.1. Pattern creation and storage

Each *pattern* consists of a sequence of *frames*, and each *frame* is a sequence of binary data specifying the activity of the LEDs for each panel. Each frame of a binary-valued pattern is created in MATLAB as a matrix consisting of zeros (corresponding to inactive pixels) and ones (corresponding to active pixels). The system also supports patterns that can display one of eight intensity levels at each pixel. Such patterns require three binary-valued matrices for each frame (see Section 2.4.1). Any pattern that can be created using this simple bitmap-like scheme can be displayed on the panels. Once a sequence of frames is created in

<sup>1</sup> <http://www.dickinson.caltech.edu/PanelsPage/>.

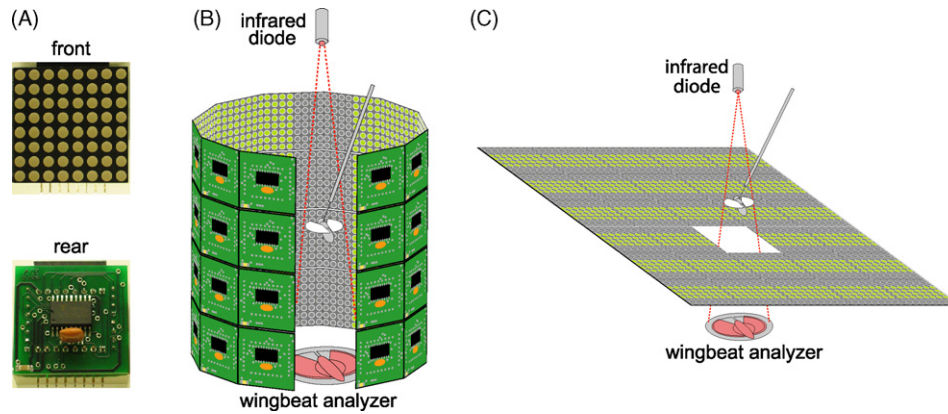


Fig. 2. The panel modules are connected to form controllable displays of varying geometries. (A) Photographs of an individual panel showing the 64-LED display. The panels are joined by 8-pin connectors: a male header on the bottom and a female header on the top of each panel. The LEDs in the dot matrix display (3 mm diameter, each), are covered with a translucent lens and are embedded in opaque black plastic. (B) To assay the sensorimotor responses of flies in rotational closed loop, the panels are configured as a flight arena, constructed as a  $4 \times 11$  cylinder of panels, height of 128 mm, diameter of 123 mm. (C) For evaluating the effect of ground motion on flight, we constructed a  $6 \times 5$  display (192 mm  $\times$  160 mm) of panels. One panel, directly below the tethered fly, is removed to allow the wingbeat shadow to project onto the sensor.

MATLAB, a program determines the portion of each frame that maps to each panel and then arranges these data into 8 bytes (or 24 for 8-level patterns). Finally, these data are ‘flattened’ into a one-dimensional array, each byte corresponding to the activation sequence for one column of one panel in one frame (3 bytes are necessary per column in the 8-level case). Because a pattern is stored as a linear array, each frame is identified by a unique index. The CF card is treated as random-access storage, so that any sequence of frames can be displayed. However, it has proven convenient to implement virtual degrees-of-freedom for the pattern data, providing the user with simple control of the sequence of frames. This alleviates the need for a complex frame-by-frame calculation to compute the next frame index. The usage of these degrees-of-freedom need not correspond to physical directions of motion. In the pattern used in the first example experiment (Section 2.6), one index is used to map the azimuthal position of a single stripe as it is rotated around the cylindrical display, and the second is used as an index into a set of contrast levels between the stripe and the background. In the second example (Section 2.7), one index maps rotations of a striped pattern, and the other maps the translation motion component. The current system implements two of these degrees-of-freedom, although it is not impossible to conceive of experiments (more complex than any that have yet been carried out with tethered insects) that would require three or more degrees-of-freedom. For example, simulating flight through a virtual two-dimensional landscape requires azimuthal rotation (about the yaw axis) and two degrees of translational motion, along the longitudinal (front-to-back, or  $Y$  axis) and the transverse (side-to-side, or  $X$  axis). Adding this functionality is a simple software extension of the pattern indexing method in the currently implemented system.

Patterns generated on a PC are stored on readily available CF cards. Even low-capacity cards can accommodate dozens of patterns. A binary image containing the patterns is copied to the CF media. At the head of the image is a sequence of slots containing information about each pattern: the number of frames, size of each frame, number of panels for this pattern,

a bit specifying whether multi-level intensities are used, and the address on the CF card where the pattern begins. After this header, the data for each frame are stored sequentially. To further optimize the speed of pattern access, the data for each frame begin at the start of a block in the CF memory.

### 2.2.2. Computer control

The PDC, and thus the display, is controlled from MATLAB through the PC’s serial port. The implemented software uses a single function for all commands that pass through the serial port. This function is called by a graphical user interface, and can also be called from the MATLAB command line or in scripts. While the PDC is running, the PC control commands can modify its operations. The supported commands allow a user to (among other options) change the current pattern, display a specific frame, set the controller mode and specify relevant runtime parameters (Section 2.3), start and stop the updating of the display, change the address of a panel, benchmark the maximal frame rate of a pattern, and update the PDC’s internal function generator. These directives can be concatenated into scripts for conducting controlled, repeatable experiments.

### 2.3. Panel display controller

The PDC coordinates the updating of the panels by reading pattern data from a CF memory card and executing commands sent by the PC control program. The PDC contains two ATmega128 (Atmel Corp.) microcontroller units (MCUs) connected to 8 analog input lines, 2 analog output lines, and 4 digital input/output lines. One MCU is dedicated to reading the pattern data from the CF card and placing it into a synchronous FIFO memory (CY7C4251V-15AC, Cypress Semiconductor Corp.). The second, or main, MCU maintains the timing of pattern updates. The software running on the main MCU decodes the commands sent from the PC control program (detailed in Section 2.2), and requests new frames from the CF-reading MCU via a dedicated serial connection. Further, the main MCU reads

the data from the FIFO buffer and transmits the appropriate part of the current frame to each panel. The PDC has been implemented such that most users can control the system directly from MATLAB with no need to modify the PDC's code. However, the PDC is fully programmable, and adaptable to future tasks. For example, the control of very complex patterns would be enabled by using multiple PDCs to control separate parts of a large display; the PDC contains a second serial port interface for just this purpose.

The PDC software has been designed to maintain fast rates of pattern data transmission from the CF card to the panels—all other tasks are handled with lower priority. There are two basic ways to control the sequence of displayed frames: the controller can determine the update rate ('velocity control'), or the frame index can be specified directly, while the timing is handled elsewhere ('position control'). A frame fetch is handled as an atomic operation; once the controller begins transmitting a certain frame, it will complete this frame before moving on to another. The maximum achievable frame rate (up to 400 Hz) thus determines the display response, since the maximum lag will be no worse than the current inter-frame interval. When the desired frame rate exceeds the achievable frame rate, the PDC will drop frames when it must, maintaining as linear a relationship between the specified frame rate and the achieved rate as is possible.

The PDC supports two *channels* of pattern control. These are the degrees-of-freedom of the memory buffer that stores the individual frames that make up a pattern. The current frame is set by the current index for both channels. To enable offline reconstruction of the time histories of the pattern indices (i.e., the sequence of displayed frames), the 2 analog outputs encode the frame index for each pattern channel. For each of these channels, several modes of control have been implemented to support a variety of fly flight experimental paradigms.

- (1) Open-loop: In this mode the current value of the internal function generator, scaled by a gain, and added to a bias, sets the display rate. The gain and bias are set in the PC control program.
- (2) Closed-loop: The difference in voltage between 2 analog input signals (scaled and offset) sets the frame update rate. In a typical tethered flight experiment, each channel is connected to a signal encoding the amplitude of each of the fly's wings.
- (3) Closed-loop with bias: This mode is a combination of the first two modes. The pattern update rate is determined by the sum of the input voltage difference (scaled by the gain), the bias, and the current function generator value. This mode is useful for supplying a time-varying bias signal to challenge a fly flying under closed-loop conditions.
- (4) External position: An input voltage sets the frame index. The gain and bias are now used to specify the mapping of the measured voltage to a frame index. This mode enables the use of an external (arbitrary) waveform generator or a second PC, etc. to set the pattern position.

- (5) Internal position: The internal function generator is used to set the current pattern frame. This is useful when precise timing of the sequence of presented frames is required.

In the 'velocity control' modes (1, 2, and 3) the PDC determines the update rate (for a certain channel) and then fetches frames sequentially at this rate. In the 'closed-loop' modes (2 and 3) this rate may be varying rapidly while the PDC is running. In the 'position control' modes (4 and 5), the displayed frame is set by an index that is either supplied by the internal software-based function generator (updated from the PC control program) or is decoded from an externally applied signal. Since the channels are updated independently, each channel can run in any one of the five modes.

#### 2.4. Display panels

The panels are the display devices of the system. Each panel is a compact package (32 mm × 32 mm × 19 mm) that contains a circuit board with an ATmega8 MCU (Atmel Corp.), an 8-channel Darlington sink driver (ULN2805), an 8 × 8 green LED dot matrix display (BM-10288MI, American Bright Optoelectronics Corp.), and other electronics for driving the LEDs (the complete schematic is shown in Fig. 3). Each panel is individually addressed and communicated with over the TWI bus (TWI is the name of Atmel's implementation of the  $I^2C$  bus, a standard interface for communication between integrated circuits). Each panel runs a compact program whose function is to receive updated pattern data and refresh the display. The brightness of each LED can be set to one of eight intensity levels, and the entire display is refreshed at no less than 372 Hz (the display rates depend on several factors, discussed in Section 4.2). The ATmega8 was selected for its low cost, small size, large number of input/output lines, integrated TWI, and the ability of each output line to directly drive an LED. While there are commercially available integrated circuit devices for driving LED displays, the programmable route taken in the design of our system yielded a faster display that is adaptable to any number of tasks.

Current is sourced from an output pin of the ATmega8 and passed through a current limiting resistor and one row of the 8 × 8 LED display. An individual LED is turned on once the corresponding column line is enabled on the Darlington driver, acting as a current sink. The distinction between the rows and columns of each panel is arbitrary; in this description we use the same convention as in the diagram of the LED matrix in the schematic (Fig. 3). The entire 64-LED matrix is scanned using 8 row lines and 8 column lines—the 'pattern' for a single column is set as the output, and then that column is enabled on the line driver. Since only one column is active at any instant in time, the LEDs must be scanned quickly to prevent the perception of flicker.

##### 2.4.1. Individual pixel intensity control

Because each panel is continuously scanned, an individual LED that is 'fully on', is in fact only receiving current during 1/8 of the refresh cycle. One refresh cycle is the time needed to update all of a panel's LED pixels. In the typical implemen-

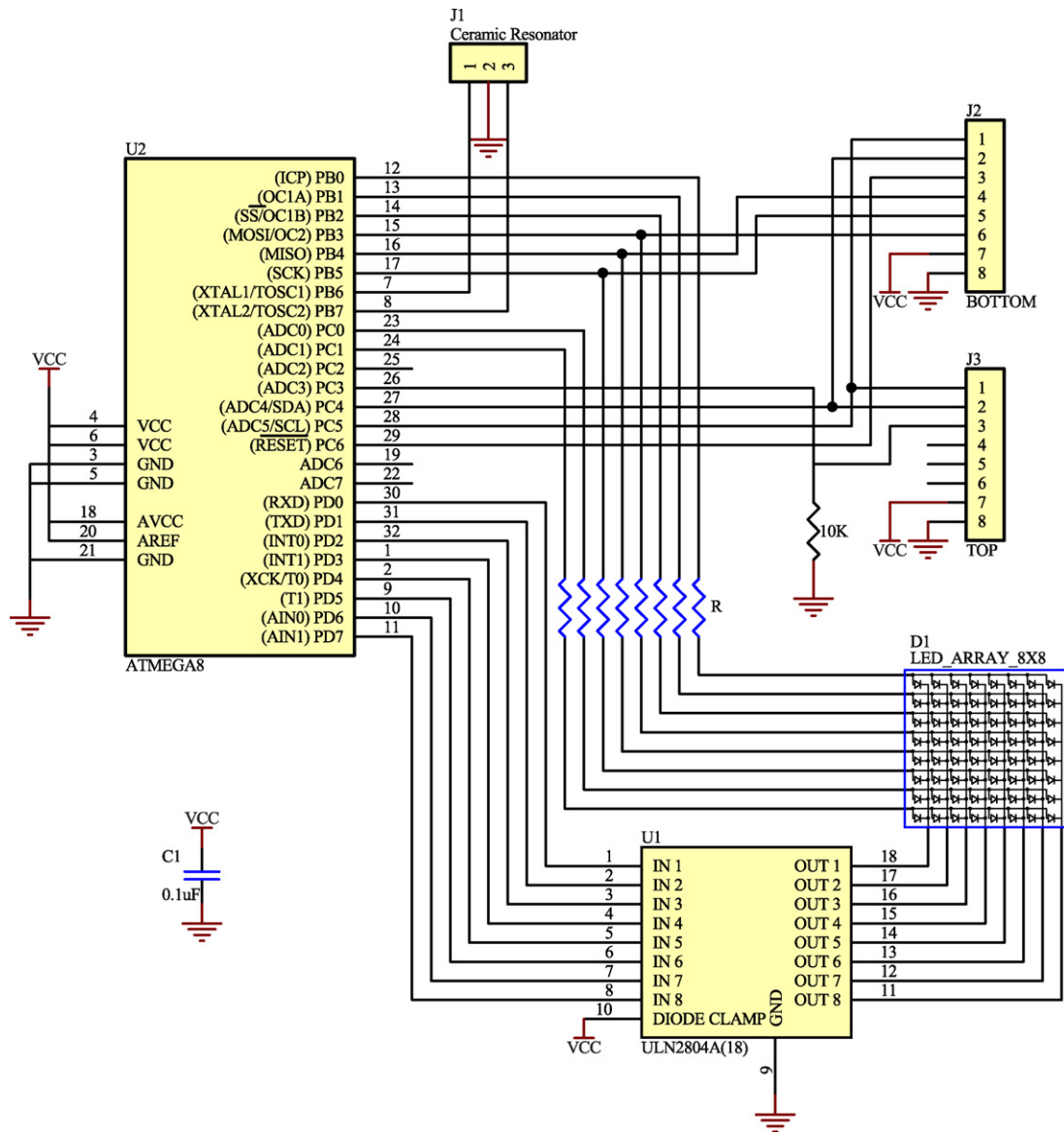


Fig. 3. Circuit schematic for one display panel. Each panel contains one Atmel ATmega8 microcontroller and an 8-channel Darlington sink driver (ULN2804A). The controller writes the pattern for one column at a time, and enables the corresponding line on the Darlington driver. The entire display is scanned by repeating this for all 8 columns. Resistors (labeled R) are used to limit the current through each row of LEDs, ensuring consistent brightness. The value of  $R$  is set to match the electrical properties of the LEDs, for our system,  $R = 82 \Omega$ . There are two 8-pin connectors, labeled *TOP* and *BOTTOM*; power, ground, and the two TWI signals pass through both connectors. Additionally, the *BOTTOM* connector carries the 3 signals necessary to program the microcontroller. Also, the  $10 \text{ k} \Omega$  pull-down resistor is used to set the RESET line of the panel connected through the *TOP* connector. Since the entire circuit board could not be larger than the  $32 \text{ mm} \times 32 \text{ mm}$  size of the LED display and the current-carrying traces must be adequate to power the display, surface mount components were used wherever possible.

tation, this cycle occurs at approximately 2600 Hz. The panels system implements multiple levels of *greenscale* intensity by using consecutive refresh cycles (each of length  $384 \mu\text{s}$ ). Using seven cycles, eight intensity levels are possible, since each LED can be on for anywhere from none to all of the refresh cycles. This scheme yields a remarkably linear control of light intensity, as demonstrated in Section 3.1. The cost of this arrangement is a reduction in the minimum refresh rate to about 372 Hz (see Section 4.2). By taking advantage of binary decoding, the system requires only 3 bytes (rather than 7) for each column of a panel's piece of a *greenscale* pattern. The panel control program extracts the 3 bits that correspond to each pixel and decodes these to obtain a value (0–7) that determines the number of refresh

cycles for which the pixel should be active. The panel controller determines how to treat the incoming packet based on its size: an 8-byte packet is a standard binary pattern and a 24-byte packet is interpreted to be an 8-level *greenscale* pattern.

### 2.5. Fly preparation

All presented experiments used 3–4-day-old female *Drosophila melanogaster*, from a laboratory culture descended from wild-caught females. The flies were maintained on a 12-h light:12-h dark cycle, and were tested during the last 5 h of their subjective day. Flies were anesthetized by cooling (to approximately  $4^\circ\text{C}$ ) and tethered to a 0.1 mm tungsten rod with

UV-activated glue. The details of the tethering procedure are as previously described in Lehmann and Dickinson (1997). In all experiments, flies were given at least 1 h of recovery, but used within 6 h. All experiments were conducted in a darkened room—the only illumination was produced by the panel displays.

### 2.6. Closed-loop experiments: object orientation

Tethered flies were positioned, in a hovering posture, in the center of a cylindrical flight arena constructed from 44 of the panels described in this paper (Fig. 2B). The panels were plugged into a circuit board that aligns 12 panels into a ring (or technically, a regular dodecagon). Eleven columns of 4 panels each were used, with one column unfilled directly behind the fly. The total resolution of this display is  $32 \times 88$  pixels. Because the display is not uniformly distant from the fly's retina, the angle subtended by each pixel on the retina depends on its height in the cylinder. The maximum size pixel for this arena geometry occurs in the coronal plane that runs through the middle of each of the fly's eyes, and subtends a visual angle of  $3.75^\circ$  on the fly's retina. This maximum pixel size is below the interommatidial distance of *Drosophila* (Heisenberg and Wolf, 1984), so pattern motion is effectively simulated as an apparent motion stimulus; the one-pixel jumps between consecutive frames produce the illusion of continuous motion. Wing motion was monitored via an optical sensor, called a 'wingbeat analyzer', described previously (Götz, 1987; Lehmann and Dickinson, 1997). The wingbeat analyzer provides an instantaneous measurement of the wingstroke amplitude of the right and left wings of the fly; these signals were connected to the analog inputs of the PDC for use in closed-loop experiments. The difference in the left and right wing stroke amplitudes is highly correlated with torque (Tammero et al., 2004), suggesting that this is an appropriate signal to use in closing a feedback loop around attempted body rotations. With the PDC set in closed-loop mode, the difference between the voltages encoding the wingbeat amplitudes was used to close a negative feedback loop around the angular velocity of a rotating pattern. All flies were positioned such that the wing beat amplitudes were within a consistent voltage range, and were run with the identical value of gain, setting the coupling between differences in left and right wingbeat amplitudes (corresponding to yaw torque) and the rotational velocity of the display. A relatively high gain was used, one that enabled all flies to readily 'fixate' a stripe within the frontal field of view, but not so large that oscillations of the stripe dominated the orientation behavior.

We sought to assess the effect of pattern intensity and contrast on the strength of stripe orientation under visual closed-loop conditions. Twenty-one combinations of stripe and background intensity were tested. A  $30^\circ$  wide vertical stripe with intensities of 0 (stripe consists of inactive LEDs), 3 (intermediate intensity level), and 7 (the brightest possible stripe consisting of maximally active LEDs), were used in combination with all background levels other than the stripe's intensity. Each combination of stripe and background intensity level is described by the *stripe contrast* of the pattern. This term is defined to be the

relative contrast between the stripe and the background:

$$\text{stripe contrast} = \frac{\text{stripe intensity} - \text{background intensity}}{\text{stripe intensity} + \text{background intensity}}$$

A positive value corresponds to a stripe that is brighter than the background, and a negative value to a background that is brighter than the stripe. The following table lists the stripe contrast for the 21 tested combinations:

Stripe intensity level	Background intensity level	Stripe contrast (%)
0	1	-100
0	2	-100
0	3	-100
0	4	-100
0	5	-100
0	6	-100
0	7	-100
3	0	100
3	1	50
3	2	20
3	4	-14.3
3	5	-25
3	6	-33.3
3	7	-40
7	0	100
7	1	75
7	2	55.6
7	3	40
7	4	27.3
7	5	16.7
7	6	7.7

Each combination was presented to tethered flies during 40-s closed-loop trials, interspersed with a 3-s pause, during which the entire display was set to a uniform, intermediate intensity value. These stimulus conditions were presented as random block trials. In total, 22 flies completed between one and two 15-min repetitions of this protocol.

### 2.7. Open-loop experiments: ground motion

Visual motion below the flies is largely absent from cylindrical arena experiments. We built a display to test the role of ground motion on the steering response of tethered *Drosophila*. Once tethered and rested, the flies were positioned in a hovering posture 6 cm above a planar configuration of the display panels. The display was constructed from 29 panels, arranged as a  $6 \times 5$  grid ( $192 \text{ mm} \times 160 \text{ mm}$ ), with one panel (directly below the fly) removed to allow for the projection of the wingbeat shadow onto the wingbeat analyzer sensor. The fly was positioned such that there was one more row of the display in front than behind her (Fig. 2C). To prevent reflections of the moving pattern from creating inadvertent motion stimuli on objects surrounding the experiment, a box lined with light-absorbing flock paper was placed around the display. The pattern consisted of alternating 4-pixel-wide bars of active and inactive pixels. In this geometry, the display is also not uniformly distant from the fly retina. Therefore, it is sensible to define the spatial and temporal frequencies of such a pattern for a hypothetical ommatidium

with an optical axis pointing straight down. Directly below the fly, the pattern has a spatial frequency of approximately  $30^\circ$ . The pattern was advanced at 5, 10, 20, and 40 frames per second, corresponding to temporal frequencies of 0.625, 1.25, 2.5, and 5 Hz, respectively (N.B. the quantity referred to here as a *temporal* frequency has historically been referred to as *contrast* frequency). Multiple orientations of the pattern were generated by rotating the original pattern frame using the Image Processing toolbox in MATLAB. Upon rotation, pixel values were determined by rounding the local intensity to force a binary-valued pattern. The experimental series consisted of a 5-s test phase of ground motion, followed by a 3-s pause with no motion, during which the entire display was set to a uniform, intermediate intensity value. During the test phase, the pattern was displayed at one of 8 orientations (cartooned along the abscissa of Fig. 6B), advancing at one of the four speeds in the direction orthogonal to the orientation of the stripes. The 32 stimulus conditions were presented in random block trials. In total, 20 flies completed between 1 and 5 repetitions of this protocol, each repetition lasting approximately 255 s.

### 2.8. Data acquisition and analysis

During the course of the experiments, the left and right wingbeat amplitudes, the wing beat frequency, and the analog voltages encoding the instantaneous positions of the 2 pattern channels were sampled at 500 Hz by a Digidata 1320A data acquisition system (Axon Instruments). Because trials were randomly determined during the course of an experiment, a USB-1208LS (Measurement Computing Corp.) was used to send a voltage encoding the current trial type from the PC script that runs each experiment. This signal was acquired along with the above data. All data analysis was performed offline using software written in MATLAB. In preparation for subsequent analysis, a data parsing routine segmented the data by trial type using the recorded signal encoding the trial identities. All

trials during which the flies stopped flying were discarded as determined by a check of the wingbeat frequency.

For the closed-loop experiments, the data set of interest is the time series of orientations of the fly, which is the rotational position record of the pattern during each trial type. We obtained a ‘summary’ of each 40-s time series (corresponding to a closed-loop stripe fixation trial at one of the 21 stripe contrast levels) by collapsing the data into an orientation histogram of 96 bins, one for each azimuthal position of the pattern.

For the open-loop ground motion experiments, the desired quantity is the mean turning response of individual flies to the short period of pattern motion. The wingbeat amplitude data was low-pass filtered (4th-order Butterworth filter, 10 Hz cutoff), and the turning response was computed as the difference between the left and right wingbeat amplitudes. For each trial, the mean response during the 250 ms previous to the stimulus onset was subtracted from the subsequent turning response. For each fly, the mean turning response was determined for each of the 32 trial types (8 directions at 4 speeds).

## 3. Results

### 3.1. Optical measurements of display properties

To characterize the optical properties of the display, the spectral intensity and the luminance of the panels were measured. The relative spectral intensity of the display was measured with a spectrometer (USB2000, Ocean Optics Inc.). This device reports the light intensity across wavelength as counts from a sensor array. Much effort and specialized equipment is required to properly convert these counts into radiometry units, so this reading was normalized and presented in arbitrary units (Fig. 4A). The reading taken when the display was inactive (intensity level of 0) was subtracted from the readings at each intensity level. These measurements show that for the 8 intensity levels that the panels are capable of displaying, only the spectral intensity increases,

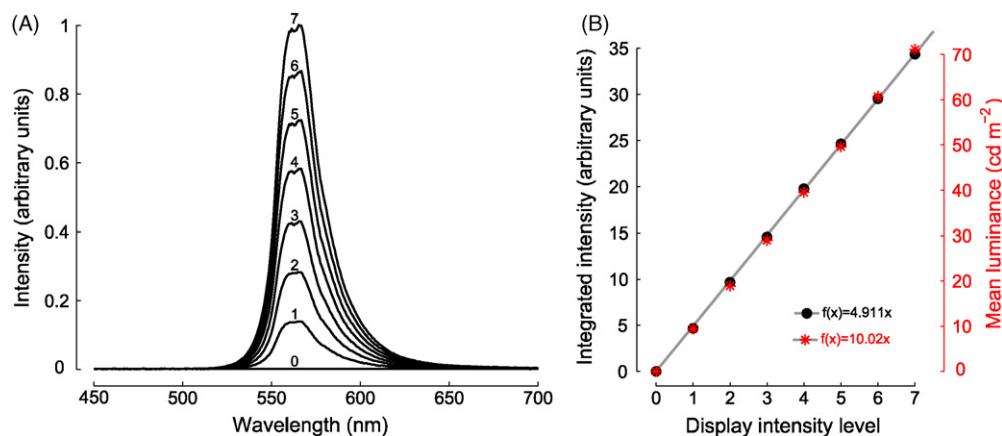


Fig. 4. The LED-based display implements 8 linearly varying intensity levels. (A) The relative intensity of the display, measured at all 8 intensity levels (numbered above each measurement), reveals that only the magnitude of the measured intensity changes, while the spectral content does not. (B) To test the scaling of the intensity levels, the measured spectral intensity response values were integrated (across wavelength) and are plotted as black circles. These values are compared to independent measurements of the absolute luminance of the surface of the display, plotted as red asterisks. Both data sets are well fit by a straight line (in gray) that passes through the origin (integrated intensity line fit:  $R^2 = 0.9999$ ; absolute luminance line fit:  $R^2 = 0.9989$ ). The ratio of the line-fit slopes is used to scale the ordinate for each set of measurements.

while the spectral content of the signal does not change. The peak in the LED intensity occurs at approximately 565 nm, corresponding to the yellow-green part of the visible spectrum. By integrating this relative intensity measurement, it is possible to estimate the success of the time-division scheme in implementing a linear set of intensity levels. The results show that the implemented system is quite linear; a least-squares line fit constrained to go through zero ( $f(x) = 4.911x$ ;  $R^2 = 0.9999$ ) is plotted along with the data (Fig. 4B). Additionally, a colorimeter (Chroma Meter CS-100A, Konica Minolta, Inc.) was used to measure the absolute luminance produced by the display. The mean absolute luminance of the display was measured at all 8 intensity levels and is also plotted in Fig. 4B. These measurements are also strikingly linear and are fit with a straight line constrained to go through zero ( $f(x) = 10.02x$ ;  $R^2 = 0.9989$ ). The integrated relative intensity and luminance data sets have been plotted on the same plot; the ratio between the slope of the line fits has been used to scale the ordinate for each data set. It is not surprising that if one data set is explained by a linear relationship, then the other will also be. Converting from radiometric to photometric quantities requires applying a wavelength-dependent scaling term (the luminous efficiency function for photopic vision) and integrating across wavelengths (Blevin et al., 1983). However, the relative magnitude between different measurements at the same wavelength will be similarly scaled, and then integrated across wavelength—these operations preserve the original relationship. The results in Fig. 4B simply show two independent confirmations of the linear scaling of the implemented intensity levels.

One parameter of interest is the maximum contrast of the display. The (Michelson) contrast is defined as the normalized difference between the luminance of the brightest and darkest regions of the display:  $(L_{\max} - L_{\min}) / (L_{\max} + L_{\min})$ , where  $L_{\max}$  and  $L_{\min}$  are the maximum and minimum luminance, respectively. Since the system is modular, the maximum contrast will largely depend on the geometry of an assembled system and the patterns being displayed. Unlike displays built from discrete LEDs, the LEDs that form the  $8 \times 8$  dot matrix displays that are used in our system are set in an opaque black plastic. This construction virtually eliminates any light bleeding from an active LED to a neighboring pixel, significantly increasing the contrast of the display. For this reason, the contrast of the 30-panel floor display (Fig. 2C) is effectively 100%. For the cylindrical flight arena (Fig. 2B), the contrast is lower due to light reflected from the opposite side of the curved display. The worst-case maximum contrast was estimated by measuring the luminance of a 16-pixel square region of the arena wall, while this region displayed a ‘fully on’ and ‘fully off’ portion of a  $30^\circ$  period striped pattern. This measurement yielded a relative contrast of approximately 93% ( $L_{\max} = 72 \text{ cd m}^{-2}$  and  $L_{\min} = 2.7 \text{ cd m}^{-2}$ ).

### 3.2. Closed-loop results: object orientation

Under closed-loop conditions, tethered *Drosophila* will vigorously orient towards a prominent vertical stripe (Heisenberg and Wolf, 1979). This behavior, termed fixation (first established in the housefly *Musca domestica* (Reichardt and Wenking, 1969)), is so robust that in a remarkable experiment, Götz (1987)

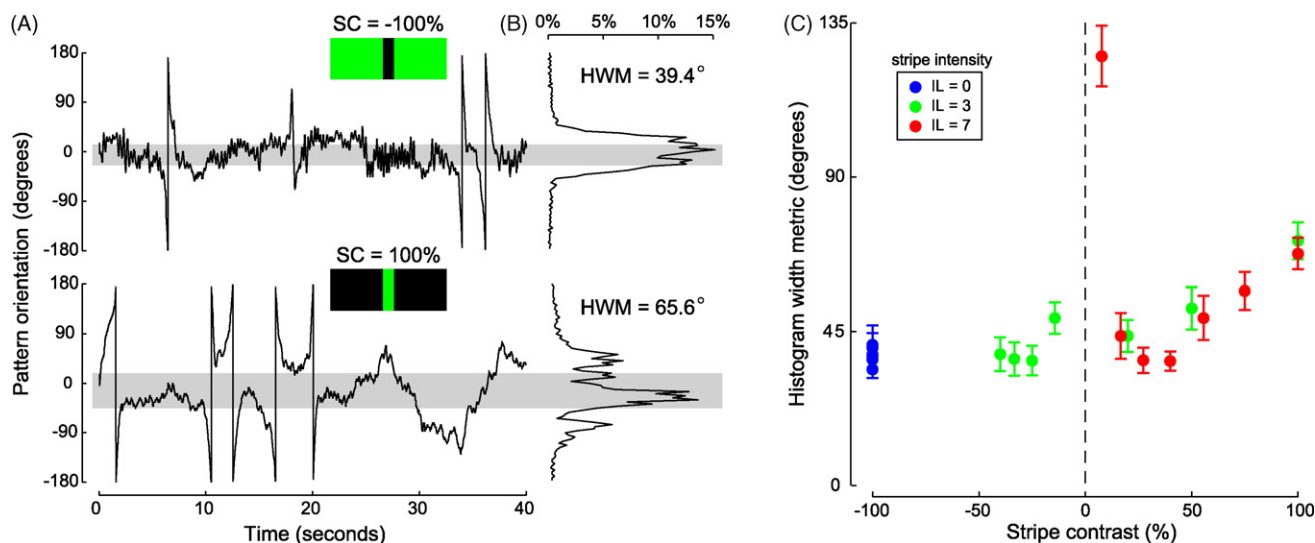


Fig. 5. The effect of pattern luminance and contrast on the closed-loop orientation behavior of *Drosophila*. (A) Example periods of orientation behavior: in the top trace the pattern is a dark stripe on a bright background (stripe contrast, SC = -100%), in the lower trace the fly was presented with a bright stripe on a dark background (SC = 100%). The fly controls the azimuthal position of the single-stripe pattern by modulating the difference between left and right wingstroke amplitudes. When the stripe is in front of the fly, the position of the pattern is near zero. (B) For each 40-s trial, the percentage of time that the flies orient towards any single position of the pattern is represented as a histogram. The gray bars correspond to the Histogram Width Metric (HWM), defined as the minimum position band that must include zero and contain 50% of the histogram area. (C) The mean ( $\pm$ S.E.M.) HWM for 21 levels of stripe contrast ( $N = 22$ ) is plotted against stripe contrast. The values are grouped by the intensity level (IL) of the stripe: blue for the lowest stripe IL, green for an intermediate stripe IL of 3 (out of 7), and red for the highest IL, corresponding to the brightest stripe. Over most of the tested range, fixation performance is nearly constant. For positive, increasing stripe contrast levels fixation degrades, evidenced by the trend towards a larger HWM. Also, clear deficits in fixation arise for the trials conducted at the lowest positive stripe contrast level.

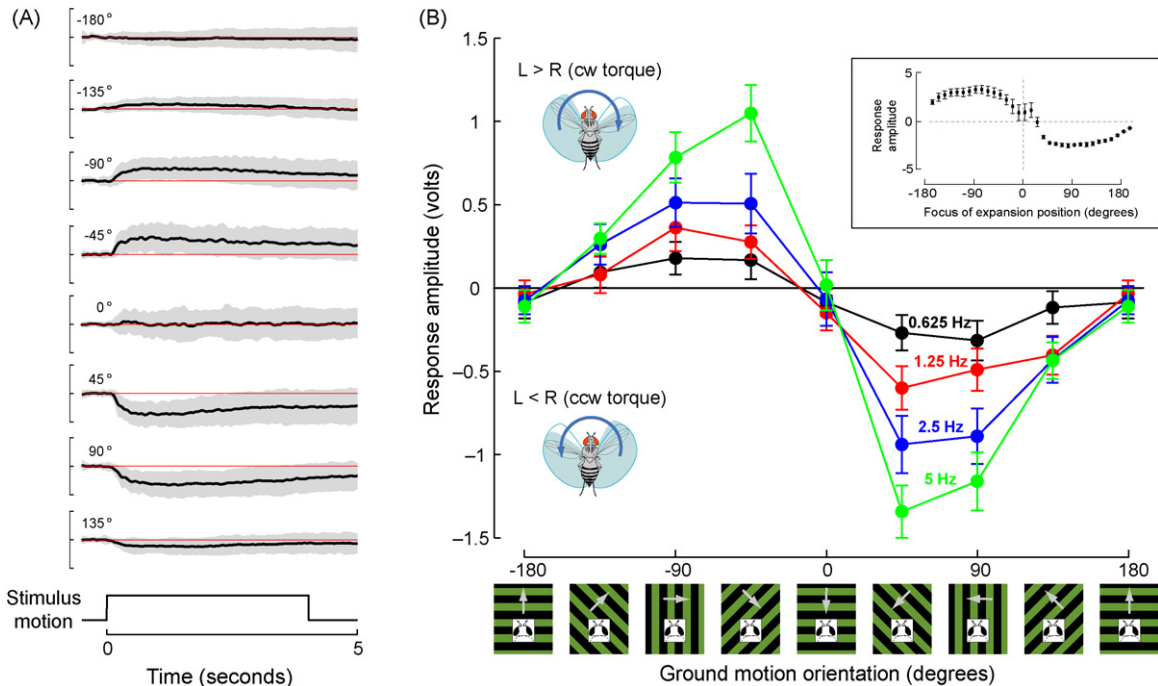


Fig. 6. The steering response of *Drosophila* to ground motion of varying speeds and orientations, presented under open-loop conditions. When presented with visual motion from below, tethered flies attempt to turn with bilateral changes in wingstroke amplitudes. (A) The turning response (difference between left and right wingstroke amplitudes) to 8 directions of ground motion, for a temporal frequency of 2.5 Hz, is displayed as mean  $\pm$  S.D. ( $N = 20$ ). The annotation on each plot corresponds to the direction of motion. The ordinate is shown as a scale reference, range is  $-2$  V to  $2$  V. (B) The mean turning response to the 4 tested temporal frequencies of ground motion is plotted against the direction of image motion ( $N = 20$ ; plotted as mean  $\pm$  S.E.M.). The diagrams of turning flies show the relationship between left (L) and right (R) wing beat amplitudes and the direction of the generated turning moment. The response curves reveal a trend that is very similar to the previous result obtained in a cylindrical arena while varying the spatial position of the focus of a panoramic stimulus of expanding stripes (inset, reproduced from Tammero et al., 2004). For the temporal frequencies tested, the responses are progressively larger for increasing temporal frequencies. The ‘tuning curve’ suggests that flies turn so as to minimize the perceived displacement of the ground beneath them.

observed sustained object orientation during a nearly continuous 32-h period. In the results presented here (Fig. 5), flies have active control over the rotational velocity of a  $30^\circ$  stripe. The position sequences of the stripe for two typical trials for an individual fly (Fig. 5A), reveal that for most of each trial, the stripe is actively positioned in front of the fly, even under inverted luminance conditions. A histogram is used to represent the percentage of time that a fly orients towards any position of the pattern (Fig. 5B). Sustained orientation towards the stripe is reflected by a large area under the histogram curve around the zero (frontal) position. By inspection, it might seem reasonable to fit the orientation histograms with a Normal distribution. However, this would be inappropriate for these data. When flies do not fixate the stripe, the pattern will often ‘spin’ around them. This spinning, when collapsed into the orientation histogram, contributes flat tails that are not well captured by a Gaussian fit. Thus, we quantify the dispersion of the orienting behavior by computing the minimum position band that includes zero, and contains 50% of the histogram area (shown as the gray bar for the two data sequences and histograms in Fig. 5A and B). The mean values ( $\pm$ S.E.M.) of the 50% histogram width metric (HWM) for the 21 tested levels of stripe contrast are shown in Fig. 5C, revealing that flies fixate stripes with nearly constant performance over a large contrast range. Further, in all cases flies truly fixate the stripe, that is, the orientation behavior is significantly different than random orientation (HWM =  $180^\circ$ ).

The blue cluster of points at  $-100\%$  contrast corresponds to the trials with a stripe of intensity 0 and the full range (1–7) of background intensity levels. For these seven conditions the fidelity of stripe fixation is essentially constant. On the right-hand side of the plot, corresponding to trials where the background is darker than the stripe, there is a noticeable trend of reduced performance with increasing stripe contrast. The one condition under which flies show clear fixation deficits (though performance still differs from random orientation), is the case of stripe intensity 7 and background intensity 6; this condition represents the highest intensity pattern with the lowest contrast (7.7%) of those tested.

The two example traces in Fig. 5A were selected because the HWM values calculated for each trial are very close to the mean for the entire set of flies. Of course, many flies do better than this mean value, and many perform worse. Because the HWM is defined to include zero, a small HWM value can only indicate that robust fixation occurs—most of the time the stripe is in front of the fly. However, several factors can contribute to a larger HWM, and large amounts of raw data must be scrutinized to determine these effects. Phenomenologically, either the pattern is spinning quickly (and thus there are insufficient motion cues to allow for stable fixation), or at other times, many flies show bouts of what has been termed ‘anti-fixation’ (Heisenberg and Wolf, 1984); the pattern is fixated for just a few seconds and then sent behind the fly, only to come up on the other side and remain

in front for a few seconds, eventually alternating sides again. A short period of ‘anti-fixation’ can be seen during the lower orientation times series in Fig. 5A (during  $t = 8\text{--}20$  s). In the conditions where fixation degrades, the orientation time series will often exhibit periods of either spinning or ‘anti-fixation’ interspersed with fixation. However, the HWM does capture the fact that for most of the tested contrast and luminance combinations, the stripe is actively positioned in front of the flies for the majority of the closed-loop trial.

### 3.3. Open-loop results: ground motion

There is evidence that visual estimation of ground motion is a crucial component of the *Drosophila* flight control system (David, 1978, 1979, 1982). We examined the response of tethered flies to motion presented from below (Fig. 6). The animal’s turning response was monitored by the optical recording of the wingbeat amplitudes on both sides of the fly. The traces in Fig. 6A show the mean ( $\pm$ S.D.) turning response of flies to coherent translatory motion (at a temporal frequency of 2.5 Hz) of the striped pattern below them. Flies turn so as to minimize the visually perceived displacement below them, e.g., when the ground is drifting from right to left (orientation of  $90^\circ$ ), the flies try to turn leftward, by producing counterclockwise torque. Therefore, the steering response to ground motion is consistent with the classically observed syndirectional optomotor turning response—when presented with a rotating environment, flies will turn so as to reduce the imposed retinal motion (Götz, 1964).

A ‘tuning’ curve for the flies’ orientation behavior (Fig. 6B) has been constructed from the aggregate mean of the per-fly mean turning responses during the first 2 s after stimulus onset, for each of the 32 trial types. For the four motion speeds that were tested, the response of flies increases with temporal frequency. Presumably, the response would saturate, and eventually decline at even higher temporal frequencies, as predicted by the response properties of insect motion detectors (Buchner, 1976). At all speeds, the mean response of flies to the moving bars oriented at  $0^\circ$  and  $180^\circ$  are close to zero. However the sign of the slope of the tuning curve through these points is opposite. This suggests that the regressive, or back-to-front, motion is the stable configuration. The stability of regressive motion predicts that flies apparently ‘prefer’ backwards flight. The shape of the tuning curve, and the predictions for stable backwards flight are highly analogous with the recently observed expansion-avoidance response (Tammero et al., 2004). For comparison this previously published tuning curve has been replicated as an inset in Fig. 6B. As has been done with the expansion-avoidance paradigm, the current results suggest that it should be possible to close a feedback loop around the direction of a translating floor stimulus.

## 4. Discussion

### 4.1. Suitability of the display for insect visual systems

The new panel-based display system described here has been designed as a stimulus source matched to the require-

ments of experiments on *Drosophila* vision. The size and resolution of each panel is such that a reasonably sized display can be constructed with a spatial resolution that is well under the interommatidial distance of *Drosophila*. Furthermore, it is possible to artificially increase the spatial resolution of a display by producing sub-pixel motion between frames, and interpolating the pixel intensities at the points of transition.

The flexibility of the developed system has enabled a variety of visual stimuli to be presented to flies. This new technology should be validated by comparing results obtained with the new system to those obtained in similar experiments with previous display methods. The results presented in Section 3.2 clearly demonstrate that in a cylindrical display of the panel modules, *Drosophila* robustly orient toward a high contrast stripe, as has been reported in numerous previous studies (e.g., Heisenberg and Wolf, 1979; Götz, 1987). In a recent set of experiments conducted with a display composed of the panel system described herein (Duistermars et al., 2007), the steering responses of tethered *Drosophila* to oscillating large-field stimuli were found to peak at a lower frequency than the responses to small field object motion, which peak at a higher oscillation frequency. This finding, while a new result for *Drosophila*, is supported by identical results found in houseflies (Egelhaaf, 1987). Finally, the new system has also been used to explore the strong expansion-avoidance response of *Drosophila*, first demonstrated in a previous version of a cylindrical LED display (Tammero et al., 2004). As previously observed, the open loop responses to large-field patterns of expansion-like motion continue to be the largest turning responses measured in *Drosophila* (as compared to large-field rotation and small field stripe motion) (Duistermars et al., 2007). In summary, the new system has allowed for the rapid reevaluation of many well-established experimental paradigms.

It is worthwhile to compare the spectral content of light emitted by the LEDs used in the display (Fig. 4A) with the spectral sensitivities measured from fly photoreceptors and from behavior. Heisenberg and Buchner (1977) showed that the relative sensitivity of the optomotor response of tethered *Drosophila* is highest for wavelengths between 350 and 500 nm, and is reduced, though still present in the greener wavelengths emitted by the panels. A similar function for the spectral sensitivity of the R1-6 photoreceptors has been measured in *Drosophila* (Wu and Pak, 1975) and other flies (Stark et al., 1977). Although the response of the *Drosophila* motion detecting system (thought to be mediated by the R1-6 retinal subsystem; see Heisenberg and Buchner, 1977) is reduced when the stimulus consists of green wavelengths, we are certain that the closed-loop stripe fixation responses (Fig. 5C) provide evidence that the brightness of the panel displays is sufficient to drive the motion detecting system to levels of saturation. Recently, blue and white LEDs have become available in the  $8 \times 8$  package that is compatible with the panel circuit. Because these LEDs will more efficiently drive the R1-6 photoreceptors, using them in future generations of the display will enable lower power consumption, and thus, larger displays dissipating less heat.

#### 4.2. Temporal control of the display

There are two independent rates to consider when discussing the performance of the display. The rate at which an individual panel refreshes all 64 pixels, is called the *refresh rate*, and the rate at which the PDC can send pattern data to the panels is called the *data rate*. Because several components of the system are programmable, it is very likely that future programming improvement will enable higher performance.

In the current system, one column of the display is illuminated according to the activation sequence in the display buffer at a rate of 20,833 Hz. The entire display is therefore refreshed at a rate of approximately 2604 Hz for a binary pattern. When a panel displays an eight-level *greenscale* pattern, seven consecutive refresh cycles are required for one *refresh* of the display, yielding a worst-case refresh rate of 372 Hz. This rate is well above the flicker fusion rate of *Drosophila* (determined by ERG recordings to be no more than 100 Hz in dark-adapted adults), and still well above the rates of most laboratory insects (Miall, 1978). The data rate also varies depending on the size of the display and the complexity of the patterns being sent. Patterns are transmitted to the panels at about 2100 eight-byte frames per second per panel. A typical cylindrical flight arena with 11 columns of panels, configured so that the panels in each column have the same address, displays approximately 190 frames per second. For a *greenscale* pattern, the increased frame size results in a data rate of approximately 68 frames per second. Several speed enhancements have been implemented. In many experiments, all rows of a panel display the identical ‘pattern’, as in the stripe fixation pattern, thus it is possible to send only one byte for a binary pattern and three bytes for a *greenscale* pattern, and have each panel simply repeat the pattern to fill all 8 rows. This approach yields roughly a five-fold speed increase. Another possibility is to buffer the patterns on each panel—there is sufficient storage to buffer 100 frames in the SRAM on each panel’s MCU. Then the PDC need only communicate the current frame number to all panels via a general call. This approach is limited in the size of the patterns for which it is appropriate, but ‘data rates’ of several kHz are possible. Furthermore, the description presented in this paper is for the most general use of the display system. There are many optimizations that could, if necessary, increase the performance of the display for a particular experiment.

#### 4.3. Contrast-dependence of object orientation behavior

In general, the absolute luminance of regions of the visual world are of little interest to the fly’s visual system. It is the difference between the luminance values of objects, the contrast, that is locally encoded by the photoreceptors and the lamina before entering the motion detecting pathway (Laughlin, 1994). Furthermore, identified motion-sensitive interneurons (in the lobula plate of the blowfly *Calliphora*) show a saturating response to motion stimuli of increasing contrast (Egelhaaf and Borst, 1989). This locally applied saturation of the contrast signal has been shown to significantly improve the accuracy of velocity estimation by models of fly Elementary Motion Detectors (EMDs;

Dror et al., 2001). The performed experiments were motivated by the presumed need of flies to be able to distinguish prominent objects in various environments under a variety of light levels. The results presented show that for most tested combinations of stripe and background luminance, the object-orientation performance of *Drosophila* is essentially constant. This finding is entirely consistent with the notion that a contrast saturation is applied to the sampled visual world, prior to the motion processing system. This saturating non-linearity enhances the contrast present in the stimulus, such that at the level of the EMDs, the stimuli are similar. However, this enhancement is not without limits: when little contrast is available in a bright scene, the motion energy caused by the moving edges that define the stripe is greatly reduced.

Our results are not without precedent. Heisenberg and Buchner (1977) recorded the closed-loop orientation behavior of tethered *Drosophila* towards a single stripe, while varying the background luminance. Their findings suggest that for increasing background luminance the frontal fixation of the stripe improves. The results presented here (Fig. 5C) do not demonstrate this effect—the HWMs for all conditions corresponding to stripes that are darker than the background are essentially equal. The simple reason for this disparity is that in the result of Heisenberg and Buchner (1977) the major improvement in the orientation behavior occurs between a background intensity of approximately  $0.01 \text{ cd m}^{-2}$  and a background intensity that is 10, 100, and 1000 times higher. However, there is only a small difference between the orientation towards a dark stripe superimposed on the two brightest backgrounds tested (approximately 1 and  $10 \text{ cd m}^{-2}$ ). The lowest (non-zero) background intensity level that we tested has a luminance of approximately  $10 \text{ cd m}^{-2}$ , which corresponds to the brightest background in the original experiment. In other related work, Heisenberg and Wolf (1979) show a surprising result—in open-loop experiments with tethered *Drosophila*, a black stripe on a white background and white stripe on a black background elicit responses of opposite polarity, suggesting that flies would orient towards the dark stripe on a bright background and away from a bright stripe on a dark background. Our results confirm that, on average, the orientation histograms of flies presented with stripes that are darker than the background (negative stripe contrast) have a lower HWM than the histograms corresponding to positive stripe contrast patterns. However, in all cases we observe that for much of the trials, flies orient towards the stripe. It is worth noting that bouts of ‘anti-fixation’ are occasionally observed (as in lower orientation sequence of Fig. 5A) during positive stripe contrast trials. A large part of the seeming discrepancy between our results and those of Heisenberg and Wolf (1979), owes to the differences in the way these experiments were conducted. Our experiments were conducted under closed loop, where the instantaneous speeds of the pattern are often quite high. In the open-loop experiment of Heisenberg and Wolf (1979), the stripe was spun around the fly at a very slow, constant rate. Further, much of the difference in orientation towards the two stimuli is seen via the turning direction implied by a train of torque spikes—short bursts of torque in one direction, thought to be the tethered flight analog of

free-flight body saccades. In high-gain, closed-loop, object-orientation experiments, torque spikes are almost entirely absent from the behaviors we record. Since the open-loop turning responses of flies are dependent on the speed, position, and direction of the stripe (Reichardt and Poggio, 1976; Heisenberg and Wolf, 1979), it is not surprising that open-loop results obtained for slow, unidirectional rotations of a stripe do not predict the behavior of flies in high-gain, closed-loop conditions.

#### 4.4. Tethered flight responses to ground motion

In the typical range of free flight body postures of *Drosophila*, large parts of the eye are pointing downwards (David, 1979, 1978); these eye regions are drastically under-stimulated in most tethered flight assays. The observed steering response of *Drosophila* when stimulated with ground motion is consistent with both the classically observed syndirectional optomotor turning response and the expansion-avoidance reflex. The response of *Drosophila* to visual motion simulating a translating flow field revealed that flies selectively orient towards the contracting pole of an expanding pattern (Tammero et al., 2004). This paradoxically suggests that flies seem to prefer flying backwards. The ground motion experiments were motivated by a desire to test the hypothesis that the lack of ground motion, known to be a critical component of the flight control system, may contribute to these paradoxical findings. This did not prove to be the case—the ground motion results are entirely consistent with the avoidance of panoramic visual expansion. In an experiment simulating side-slip, a tethered fly in a cylindrical flight arena, presented with an expansion cue to their right, will try to turn leftwards (Tammero et al., 2004). The corresponding global side-slip stimulus would consist of right-to-left ground motion, from which we show that flies would also turn leftwards. It is almost certain that the combined stimulus (presented in a hypothetical cylindrical flight arena above a floor display) would elicit responses of the same direction.

To our knowledge, these experiments were the first attempt to measure the response of a tethered fly to pattern motion presented from below the animal. With freely flying *Drosophila* in a wind tunnel, David (1979) showed that for strong ground motion stimuli, most flies exhibit floor-following speed changes. If the floor is accelerated below them, then flies modulate their airspeed to move in the direction of the ground motion. However, in these results, flies maintained their upwind orientation, and moved relative to the ground motion by modulating their production of forward thrust. In a separate experiment, flying *Drosophila* in still air were found to orient in the direction of moving stripes presented in a square opening in the floor of a square chamber (David, 1982). While our results show a type of floor-following behavior, the tuning curve presented in this paper predicts that flies should orient so that they receive a regressive ground cue. David (1979, 1982) does not report this behavior; presumably the role of wind, or some other sensory stimulus not present under tethered conditions, is sufficient to bias the flies' orientation towards progressive motion.

#### 4.5. Future work

The display panels are presented as a very useful, completed design. However, several improvements can be made to the PDC that would further extend the flexibility of the system. Sensible future modifications include a VGA or DVI interface for streaming images from a PC video card to the panels, and support for multiple TWI buses for driving larger displays. A trivial modification that will yield increased performance is to replace the Atmel MCUs used in both the panels and the PDC with compatible, but faster components, as they become available.

### 5. Conclusions

The display system has now been in use in our laboratory for over 2 years and has proved to be a robust experimental instrument. These devices have even withstood the abuses of intense usage during a two-week laboratory cycle as part of the Neural Systems and Behavior course at the Marine Biological Laboratory over the past two summers. The modularity and low cost of the system make it ideal for a wide variety of laboratory applications in both research and education. In addition to the two display configurations presented here, at least six other display types have been assembled and used for behavioral or electrophysiological experiments. The addition of a controllable visual display to virtually any fly behavior experiment – even those pursuing a non-visual question – has time and again proven to be a successful strategy.

### Acknowledgements

The authors wish to thank Robert Bailey for invaluable help in the electronic design, Shinsuke Shimojo for use of his laboratory's colorimeter, and Mark Frye and Wyatt Korff for their insightful editing. This work was supported by the Institute for Collaborative Biotechnologies through grant DAAD19-03-D-0004 from the US Army Research Office and by the CNSE Engineering Research Center at Caltech through NSF award EEC-9402726.

### References

- Blevin WR, Kessler K, Mielenz KD, Wyszecki G. Principles governing photometry. *Metrologia* 1983;19(3):97–101.
- Buchner E. Elementary movement detectors in an insect visual system. *Biol Cybern* 1976;24(2):85–101.
- David CT. Relationship between body angle and flight speed in free-flying *Drosophila*. *Physiol Entomol* 1978;3(3):191–5.
- David CT. Optomotor control of speed and height by free-flying *Drosophila*. *J Exp Biol* 1979;82:389–92.
- David CT. Competition between fixed and moving stripes in the control of orientation by flying *Drosophila*. *Physiol Entomol* 1982;7(2):151–6.
- Dror RO, O'Carroll DC, Laughlin SB. Accuracy of velocity estimation by reichardt correlators. *J Opt Soc Am A* 2001;18(2):241–52.
- Duistermars BJ, Reiser MB, Zhu Y, Frye MA. Dynamic properties of large-field and small-field optomotor flight responses in *Drosophila*. *J Comp Physiol A* 2007;193(7):787–99.
- Egelhaaf M. Dynamic properties of two control-systems underlying visually guided turning in houseflies. *J Comp Physiol A* 1987;161(6):777–83.

- Egelhaaf M, Borst A. Transient and steady-state response properties of movement detectors. *J Opt Soc Am A* 1989;6(1):116–27.
- Götz KG. Optomotorische untersuchung des visuellen systems einiger augenmutanten der fruchtfliege *drosophila*. *Kybernetik* 1964;2(2):77–91.
- Götz KG. Flight control in *Drosophila* by visual perception of motion. *Kybernetik* 1968;9:159–82.
- Götz KG. Course-control, metabolism and wing interference during ultralong tethered flight in *Drosophila melanogaster*. *J Exp Biol* 1987;128:35–46.
- Hausen K. Motion sensitive interneurons in the optomotor system of the fly. 1. The horizontal cells: structure and signals. *Biol Cybern* 1982;45(2):143–56.
- Heisenberg M, Buchner E. Role of retinula cell-types in visual behavior of *Drosophila melanogaster*. *J Comp Physiol A* 1977;117(2):127–62.
- Heisenberg M, Wolf R. On the fine-structure of yaw torque in visual flight orientation of *Drosophila melanogaster*. *J Comp Physiol A* 1979;130(2):113–30.
- Heisenberg M, Wolf R. *Vision in Drosophila*. Berlin: Springer Verlag; 1984.
- Krapp HG, Hengstenberg R. A fast stimulus procedure to determine local receptive field properties of motion-sensitive visual interneurons. *Vision Res* 1997;37(2):225–34.
- Laughlin SB. Matching coding, circuits, cells, and molecules to signals: general principles of retinal design in the fly's eye. *Prog Retin Res* 1994;13(1):165–95.
- Lehmann FO, Dickinson MH. The changes in power requirements and muscle efficiency during elevated force production in the fruit fly *Drosophila melanogaster*. *J Exp Biol* 1997;200(7):1133–43.
- Lindemann JP, Kern R, Michaelis C, Meyer P, van Hateren JH, Egelhaaf M. Flimax, a novel stimulus device for panoramic and highspeed presentation of behaviourally generated optic flow. *Vision Res* 2003;43(7):779–91.
- Liu G, Seiler H, Wen A, Zars T, Ito K, Wolf R, Heisenberg M, Liu L. Distinct memory traces for two visual features in the *Drosophila* brain. *Nature* 2006;439(7076):551–6.
- Miall RC. Flicker fusion frequencies of 6 laboratory insects, and response of compound eye to mains fluorescent ripple. *Physiol Entomol* 1978;3(2):99–106.
- Reichardt W. Autocorrelation, a principle for the evaluation of sensory information by the central nervous system. In: Rosenblith W, editor. *Sensory communication*. New York: MIT Press; 1961. p. 303–17.
- Reichardt W, Poggio T. Visual control of orientation behavior in fly. 1: Quantitative analysis. *Q Rev Biophys* 1976;9(3):311–75.
- Reichardt W, Wenking H. Optical detection and fixation of objects by fixed flying flies. *Naturwissenschaften* 1969;56(8):424–5.
- Stark WS, Ivanyshyn AM, Greenberg RM. Sensitivity and photopigments of r1–6, a 2-peaked photoreceptor, in *Drosophila calliphora* and *Musca*. *J Comp Physiol A* 1977;121(3):289–305.
- Strauss R, Schuster S, Götz KG. Processing of artificial visual feedback in the walking fruit fly *Drosophila melanogaster*. *J Exp Biol* 1997;200(9):1281–96.
- Tammero LF, Frye MA, Dickinson MH. Spatial organization of visuomotor reflexes in *Drosophila*. *J Exp Biol* 2004;207(1):113–22.
- Von Holst E, Mittelstaedt H. Das reafferenzprinzip. *Naturwissenschaften* 1950;37(20):464–76.
- Wu CF, Pak WL. Quantal basis of photoreceptor spectral sensitivity of *Drosophila melanogaster*. *J Gen Physiol* 1975;66(2):149–68.